ARCHIVES OF ELECTRICAL ENGINEERING VOL. 68(1), pp. 15–32 (2019)

DOI 10.24425/aee.2019.125977

Multi-objective coordination optimisation method for DGs and EVs in distribution networks

HUILING TANG[1,2], JIEKANG WU[1]

[1] *School of Automation, Guangdong University of Technology, China*

[2] *School of Physics & Optoelectronic Engineering, Guangdong University of Technology, China*
e-mail: wujiekang@163.com

(Received: 11.01.2018, revised: 17.09.2018)

Abstract: The loss of power and voltage can affect distribution networks that have a significant number of distributed power resources and electric vehicles. The present study focuses on a hybrid method to model multi-objective coordination optimisation problems for distributed power generation and charging and discharging of electric vehicles in a distribution system. An improved simulated annealing based particle swarm optimisation (SAPSO) algorithm is employed to solve the proposed multi-objective optimisation problem with two objective functions including the minimal power loss index and minimal voltage deviation index. The proposed method is simulated on IEEE 33-node distribution systems and IEEE-118 nodes large scale distribution systems to demonstrate the performance and effectiveness of the technique. The simulation results indicate that the power loss and node voltage deviation are significantly reduced via the coordination optimisation of the power of distributed generations and charging and discharging power of electric vehicles. With the methodology supposed in this paper, thousands of EVs can be accessed to the distribution network in a slow charging mode.

Key words: charging and discharging of electric vehicles, distribution networks, distributed generation, multi-objective coordination optimisation, SAPSO

1. Introduction

Recently, increasing concerns related to the greenhouse effect and the shortage of traditional energy resources including coal, oil, and gas have increased distributed generations (DGs) in distribution networks. The DGs, such as hydropower, wind energy, solar energy, and storage power stations, are favoured by individuals due to their clean, renewable, and efficient characteristics [1–3]. Simultaneously, electric vehicles (EVs) are expected to play a major role in transportation electrification given their reduction in emission of greenhouse gases. However, large-scale access of EVs and DGs inevitably creates several challenges in the planning and operations of distribution networks. Therefore, a critical issue that should be urgently resolved corresponds to methods to coordinate the power generation of DGs and charge and discharge power of EVs in distribution networks.

Numerous studies significantly contributed to investigating the location and capacity of DGs [4–7]. Additionally, significant research attention also focused on methods to optimise the planning of charging stations for EVs [8–12]. Nevertheless, most extant studies considered the impact of the access for either only DGs or only EVs and did not consider the interaction between DGs and EVs when they simultaneously access the distribution networks [13–19]. Specifically, the influence of the access to DGs and EVs in the distribution networks significantly differs from that when only DGs or EVs access the operation of the distribution networks. Recently, a few extant studies examined the coordination of DGs and EVs in the distribution networks [20–24]. Li *et al*. [20] considered the operating cost of distribution companies, investment cost of DGs investors, environmental benefit of DGs, and grid investment savings by vehicle to grid (V2G). Additionally, a mathematical model for DGs optimal planning in distribution networks involving EVs was developed based on chance constrained programming with a hybrid coding based improved adaptive genetic algorithm to solve the model. Chen *et al*. [21] proposed a novel chance-constrained optimal reconfiguration model for a distribution system and analysed the uncertainty of load and DGs and charging/discharging strategy of a plug-in electric vehicle (PEV) while considering power loss minimisation as the objective function. In [22], a model to determine the site and capacity of DGs and EV charging stations (in which the minimum total cost, lowest network loss, and highest traffic satisfaction were considered as objectives) was constructed and solved via a new multi-objective free-search algorithm. In [23] considering the temporal and spatial uncertainties that are associated with stochastic generation, traditional demand, and EV charging loads, a series of generation-demand scenarios were constructed, and a two-stage planning model for optimal siting and sizing DG and intelligent parking lots was developed while considering the minimisation of system construction and operation cost as the goal. Awasthi *et al*. [24] focused on the optimal planning (sitting and sizing) of charging station infrastructure in the city of Allahabad, India. The objective function considers the economic aspects of station setup including land cost, station equipment, and operating and maintenance costs. However, extant studies only considered the cost of power loss in the planning period or the cost of investment and construction and did not consider voltage deviation in the distributed networks when DGs and EVs access the power grid.

In the study, the effect of DGs and EVs on voltage deviation and power loss in distribution networks are considered. The power loss and voltage deviation in the traditional network and distribution networks with DGs and EVs are compared and analysed. Additionally, a mathematical model that includes the power loss index and voltage deviation index of the distribution networks with DGs and EVs is obtained. Finally, a multi-objective optimisation model with a minimum power loss index and a low voltage deviation index is established to coordinate and optimise the power generation of DGs and charging and discharging power of EVs in the distribution networks.

2. Multi-objective optimisation model for DGs generation and charging and discharging of EVs

2.1. The calculation of power loss of distribution networks with DGs and EVs

It is assumed that the DGs and EVs are accessed at different nodes of the distribution networks as shown in Fig. 1.

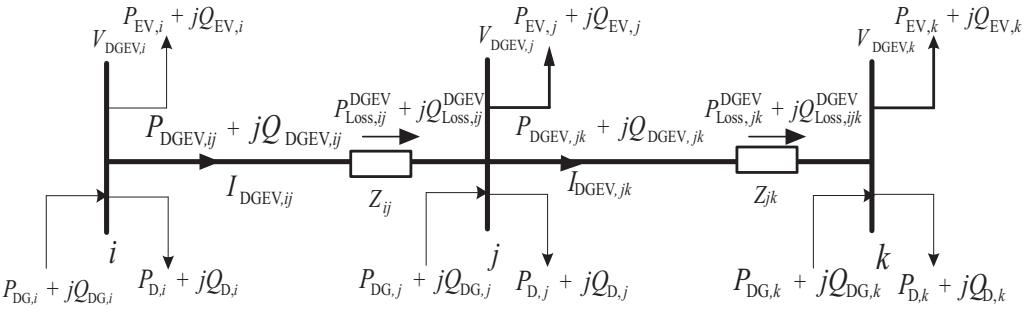

Fig. 1. Node i, j, k in a distribution network with DGs and EVs

As shown in Fig. 1, it is assumed that $V_{\mathrm{DGEV},j}$ denotes the node voltage of node j in distribution networks with DGs and EVs, $I_{\mathrm{DGEV},ij}$ denotes the branch current flowing through branch ij in distribution networks with DGs and EVs, $P_{\mathrm{DGEV},ij}$ and $Q_{\mathrm{DGEV},ij}$ denote active power and reactive power, respectively, on branch ij in the distribution networks with DGs and EVs; $P^{\mathrm{DGEV}}_{\mathrm{Loss},ij}$ and $Q^{\mathrm{DGEV}}_{\mathrm{Loss},ij}$ denote active power loss and reactive power loss, respectively, on branch ij in the distribution networks with DGs and EVs; $P_{\mathrm{DG},j}$ and $Q_{\mathrm{DG},j}$ denote active power and reactive power, respectively, as provided by DGs; and $P_{\mathrm{EV},j}$ and $Q_{\mathrm{EV},j}$ denote active power and reactive power, respectively, as provided by EVs. Additionally, an EV is in the charged state when $P_{\mathrm{EV},j}$ is positive. When $P_{\mathrm{EV},j}$ is negative, the electric vehicle is in a discharge state. Additionally, when $P_{\mathrm{EV},j}$ is 0, it indicates that the electric vehicle is neither in the charge state or discharge state.

Furthermore, P_{TLoss} is defined as the total power loss of the traditional distribution networks; and P_{TLoss} is obtained as (1).

$$P_{\mathrm{TLoss}} = \sum_{ij \in S_l} P_{\mathrm{Loss},ij}\,, \tag{1}$$

where $P_{\mathrm{Loss},ij}$ denotes the active power loss on branch ij in the traditional distribution networks. The total power loss of the distribution networks with DGs and EVs is obtained from (2) [25].

$$P^{\mathrm{DGEV}}_{\mathrm{TLoss}} = \sum_{ij \in S_l} P^{\mathrm{DGEV}}_{\mathrm{Loss},ij}\,. \tag{2}$$

2.2. Power loss index (*PLI*)

With respect to the distribution networks with DGs and EVs, k_{PLI} is defined as the power loss index of the whole distribution networks with DGs and EVs. Specifically, k_{PLI} is used to measure the impact on the power loss of distribution networks given that DGs and EVs access the distribution networks [25]. Additionally, the k_{PLI} is expressed as

$$k_{PLI} = \frac{P^{\mathrm{DGEV}}_{\mathrm{TLoss}}}{P_{\mathrm{TLoss}}}\,. \tag{3}$$

Based on (3), if k_{PLI} decreases, then it implies that the total power loss of the distribution networks with DGs and EVs is lower than that in the traditional distribution networks.

2.3. Voltage deviation index (*VDI*)

In the distribution networks, voltage is an important index to evaluate power quality and to check the security of the system. Given the existence of a load, the voltage drop increases when the distance between node and substation increases. Additionally, this leads to voltage deviations in a few nodes of the distribution networks, and this affects the normal operation of the system. With decreases in the voltage, the power loss of the system also increases. Therefore, if the DGs and EVs access the distribution networks on a large scale, then they inevitably affect the voltage deviation of the distribution networks. However, the voltage deviation of each node is significantly reduced when the power of the DGs and the charge and discharge power of the EVs are properly coordinated. Hence, k_{VDI} is defined as the voltage deviation index of the whole distribution networks with DGs and EVs.

$$k_{VDI} = \frac{\sum\limits_{j \in S_b} \left|\Delta V_{\mathrm{DGEV},j}\right|}{\sum\limits_{j \in S_b} \left|\Delta V_j\right|} = \frac{\sum\limits_{j \in S_b} \left|V_{\mathrm{DGEV},j} - V_0\right|}{\sum\limits_{j \in S_b} \left|V_j - V_0\right|}, \tag{4}$$

where V_0 denotes the rated voltage, and S_b denotes the collection of all nodes of the distribution networks. Evidently, as given in (4), k_{VDI} is a fraction. The numerator of k_{VDI} denotes the total absolute value of the voltage deviation of all nodes in the distribution networks with DGs and EVs. The denominator of k_{VDI} denotes the total absolute value of the voltage deviation of all nodes in traditional distribution networks.

2.4. Multi-objective optimisation model

The following section describes a multi-objective coordinated optimisation model for the power of DGs and charging and discharging power of EVs.

2.4.1. Objective function

The multi-objective coordination optimisation model [26] involves minimising the power loss index k_{PLI} and voltage deviation index k_{VDI}. The model is transformed in the form of proportional coefficients without units, and thus the aforementioned two target optimisation models are directly weighted to obtain the multi-objective optimisation function. The objective function F is represented as

$$\text{Minimize } F = (\gamma_1 k_{PLI} + \gamma_2 k_{VDI}), \tag{5}$$

where γ_1 and γ_2 are weight factors. And

$$\sum_{q=1}^{2} \gamma_q = 1.0 \ \wedge \ \gamma_q \in [0, 1], \tag{6}$$

In the study, a multi-objective comprehensive evaluation method analytic hierarchy process AHP is adopted [27], and this determines the optimal weight coefficient of each sub goal in the multi-objective function. First, a pairwise comparison matrix is composed of the scale from 1 to 9

after comparing the importance of each of the two indices (in this paper, indices refer to k_{PLI} and k_{VDI}). The more important of the index is, the larger scale value is associated to it. A pairwise comparison matrix can be expressed as following:

$$B = \left[\begin{array}{c|cccc} & B_1 & B_2 & \cdots & B_n \\ \hline B_1 & b_{11} & b_{12} & \cdots & b_{1n} \\ B_2 & b_{21} & b_{22} & \cdots & b_{2n} \\ \vdots & \vdots & \vdots & \ddots & \vdots \\ B_n & b_{n1} & b_{n2} & \cdots & b_{nn} \end{array}\right], \tag{7}$$

where $\boldsymbol{B}_i$ represents the index i and n is the number of indices; b_{ij} represents the importance comparison result between $\boldsymbol{B}_i$, $\boldsymbol{B}_j$ and $b_{ij} = 1/b_{ji}$ $(i, j = 1, 2, \cdots n)$.

$b_{ii} = 1$ $(i = 1, 2, \cdots, n)$ represents the importance comparison result between the index $\boldsymbol{B}_i$ and itself.

Then the weighting coefficient W_i for each index can be calculated from

$$W_i = \frac{\sqrt[n]{\prod_{j=1}^{n} b_{ij}}}{\sum_{i=1}^{n} \overline{W_i}} \quad (i = 1, 2, \cdots, n). \tag{8}$$

$\boldsymbol{W} = [W_1 \;\; W_2 \;\; \cdots \;\; W_n]^T$ represents the eigenvectors of the pairwise comparison matrix $\boldsymbol{B}$.

Finally, checking the consistency of the pairwise comparison matrix $\boldsymbol{B}$ as following:

$$CR = \frac{(\lambda_{\max} - n)}{(n-1) \cdot RI} < 0.1, \tag{9}$$

where: CR is the consistency ratio, if $CR < 0.1$, that means the weighting coefficient of each index is reasonable. n is the index number. RI is the random index, and its values are given in [28]. $\lambda_{\max}$ is the maximal eigenvalue of $\boldsymbol{B}$.

$$\lambda_{\max} = \sum_{i=1}^{n} \frac{(\boldsymbol{B}\,\boldsymbol{W})_i}{nW_i}. \tag{10}$$

In this paper, from the perspective of Power Grid Corp's economy, it is necessary to minimize the power loss of each branch in distribution networks and ensure the voltage deviation within the limit [29]. That means that reducing the power loss of each branch is more important than decreasing the voltage deviation of each node in the distribution network. So the scale value for k_{PLI} and k_{VDI} in the AHP is 3 and 1. Thus, the pairwise comparison matrix is formed as follows:

$$\boldsymbol{B} = \left[\begin{array}{c|cc} & k_{PLI} & k_{VDI} \\ \hline k_{PLI} & 1 & 3 \\ k_{VDI} & 1/3 & 1 \end{array}\right]. \tag{11}$$

Based on [30], the optimal weighting coefficients of the two indices in the objective function (5) are set $\gamma_1 = 0.7$, $\gamma_2 = 0.3$ and the consistency ratio $CR = 0 < 0.1$.

2.4.2. The constraint conditions

1) The equality constraint conditions of active and reactive power are expressed as:

$$\begin{cases} \sum\limits_{j\in S_b} P_{\mathrm{DG},j} + P_S = \sum\limits_{j\in S_b} (P_{\mathrm{EV},j} + P_{\mathrm{D},j}) + P_{\mathrm{TLoss}}^{\mathrm{DGEV}} \\ \sum\limits_{j\in S_b} Q_{\mathrm{DG},j} + Q_S = \sum\limits_{j\in S_b} (Q_{\mathrm{EV},j} + Q_{\mathrm{D},j}) + Q_{\mathrm{TLoss}}^{\mathrm{DGEV}} \end{cases}, \tag{12}$$

where P_S and Q_S denote active power and reactive power provided by the main network, respectively.

2) Inequality constraint conditions:

a) Power constraint conditions for the distributed power supplies

$$\begin{cases} P_{\mathrm{DG}}^{\min} \le P_{\mathrm{DG},j} \le P_{\mathrm{DG}}^{\max} \\ Q_{\mathrm{DG}}^{\min} \le Q_{\mathrm{DG},j} \le Q_{\mathrm{DG}}^{\max} \end{cases}, \tag{13}$$

where $P_{\mathrm{DG}}^{\max}$ and $P_{\mathrm{DG}}^{\min}$ denote the upper and lower limits, respectively, of DGs' active power, $Q_{\mathrm{DG}}^{\max}$ and $Q_{\mathrm{DG}}^{\min}$ denote the upper and lower limits, respectively, of DGs' reactive power.

b) The charge and discharge power constraints of the electric vehicle

$$\begin{cases} -P_{\mathrm{EV}}^{\mathrm{Dmax}} \le P_{\mathrm{EV},j} \le P_{\mathrm{EV}}^{\mathrm{Cmax}} \\ -Q_{\mathrm{EV}}^{\mathrm{Dmax}} \le Q_{\mathrm{EV},j} \le Q_{\mathrm{EV}}^{\mathrm{Cmax}} \end{cases}, \tag{14}$$

where $-P_{\mathrm{EV}}^{\mathrm{Dmax}}$ and $-Q_{\mathrm{EV}}^{\mathrm{Dmax}}$ denote the maximum discharging active power and reactive power, respectively, of EVs, and $P_{\mathrm{EV}}^{\mathrm{Cmax}}$ and $Q_{\mathrm{EV}}^{\mathrm{Cmax}}$ denote the maximum active power and reactive power, respectively, as obtained by EVs from distribution networks.

c) Constraints of node voltage

$$V^{\min} \le \left|V_{\mathrm{DGEV},j}\right| \le V^{\max}, \tag{15}$$

where $V^{\max}$ and $V^{\min}$ denote the upper and lower limits, respectively, of the node voltage of node j.

d) Branch current and power flow constraints

$$\left|I_{\mathrm{DGEV},ij}\right| \le \left|I_{ij}^{\max}\right|, \tag{16}$$

$$\begin{cases} P_{\mathrm{DGEV},ij} \le P_{ij}^{\max} \\ Q_{\mathrm{DGEV},ij} \le Q_{ij}^{\max} \end{cases}, \tag{17}$$

where $I_{ij}^{\max}$ denotes the upper limit of the current flowing through branch ij, and $P_{ij}^{\max}$ as well as $Q_{ij}^{\max}$ denote the upper limits of active power and reactive power, respectively, of branch ij.

3. Solution

3.1. Particle swarm optimisation algorithm

The particle swarm optimisation (PSO) algorithm [31] is a new evolutionary algorithm that is recently developed. It uses individual information in a group to share information, and thus the movement of the whole group evolves from disorder to order in the solution space. The optimal solution is obtained. The evolution process is as follows:

$$v_{i,j}(t+1) = \omega v_{i,j}(t) + c_1 r_1 (p_{i,j} - x_{i,j}(t)) + c_2 r_2 (p_{g,j} - x_{i,j}(t)), \tag{18}$$

$$x_{i,j}(t+1) = x_{i,j}(t) + v_{i,j}(t+1), \tag{19}$$

where ω denotes the inertia weight factor, c_1 and c_2 denote positive learning factors, r_1 and r_2 denote random numbers uniformly distributed in [0, 1], $p_{i,j}$ denotes the local optimum position vector of particle i, and $p_{g,j}$ denotes the global optimum position vector for all particles. Additionally, $v_{i,j}(t)$ and $x_{i,j}(t)$ correspond to the j dimensional velocity vectors and position vectors of the particle i, and this evolves into the t generation. The PSO is widely used in various optimisation problems due to its simple structure, fast convergence, and easy implementation. However, when the model is complex, in the course of evolution and especially in the later stage of evolution, populations tend to lose diversity and fall into local optima because the learning factor and inertia weight factor are constant. It is difficult to obtain the global optimal solution. Therefore, several recent studies focused on improving the PSO algorithm. A few achievements are achieved including a few improvements in the application of in power systems [32].

3.2. Simulated annealing particle swarm optimisation

The simulated annealing (SA) algorithm [33] is a stochastic optimisation algorithm based on a Monte-Carlo evolutionary solution strategy, and this is based on the similarity between the annealing process of the solid substance and general combinatorial optimisation problem. The global optimal solution of the objective function is randomly searched for in the solution space using the probability jump characteristics. Thus, it jumps out of the local optimum and finally tends to the global optimum. The combination of the SA algorithm and PSO effectively overcomes the disadvantage of the PSO wherein it easily falls into local optimum.

The SAPSO algorithm steps are as follows:

1) Initialisation: the number of populations and times of evolution are defined, and the positions and velocities of each particle are randomly generated.

2) Fitness evaluation, the local optimum position of particles p_i, and global optimum position p_g are updated.

3) The initial temperature is determined.

4) The roulette wheel strategy is used to determine the new global surrogate value p'_g from all the p_i values and subsequently the speed and position of each particle is updated based on (18) and (19).

$$\omega = \omega_{\max} - t(\omega_{\max} - \omega_{\min})/t_{\max}, \tag{20}$$

where $\omega_{\max}$ and $\omega_{\min}$ denote the maximum and minimum values, respectively, of the inertia weight factor, and $t_{\max}$ denotes the maximum number of iterations.

To improve the ability of local search and the global search ability of the particle swarm algorithm in the process of evolution, the inertia weight factor is adjusted dynamically online,

and thus the inertia weight factor decreases from a maximum to a minimum. The relationship between the numbers of iterations of the algorithm is as follows:

5) The new fitness value of each particle is calculated and subsequently the value of each particle p_i and value of population p_g are updated.

6) The crossover of the newly generated particle swarm is performed by probability P_c. We recalculate the objective function of the new particles. The formula of the offspring after cross operation based on SA is as follows:

$$\text{Minimize}\left\{1,\ e^{-(f(x_j')-f(x_j))/T}\right\} > r_{\text{and}}, \tag{21}$$

$$\text{Minimize}\left\{1,\ e^{-(f(x_k')-f(x_k))/T}\right\} > r_{\text{and}}, \tag{22}$$

where $f(x_i)$ and $f(x_k)$ denote the pre-cross fitness of particles, $f(x_i')$ and $f(x_k')$ denote the fitness of particles after crossing and, r_{and} denotes a random number in (0–1). A new entity satisfying (21) and (22) is accepted and replaced by the original individual.

7) The new particle swarm generated by crossover operation is mutated by probability P_m. The acceptance formula of the offspring after mutation based on SA is identical to that in the cross operation. We recalculate the objective function of the new particles. A new entity that satisfies (21) and (22) is accepted and replaced by the original individual.

8) Annealing is performed based on the following formula:

$$T(t+1) = \alpha T(t), \tag{23}$$

where $T(t)$ denotes the annealing temperature for the evolution of the t generation, and α denotes the cooling coefficient wherein the number is between (0–1).

9) If the number of times of evolution is satisfied, then the algorithm ends and the output turns, and otherwise it turns to 4.

4. Example analysis

4.1. Related data assumptions and requirements

To verify the model and method proposed, the IEEE-33 node distribution system is considered as an example to perform simulations and analysis. The active power, reactive power, and resistance of each node in the system are per unit values and related to the capacity of 10 MVA and the voltage of 12.66 kV [25]. A few assumptions are proposed for the example analysis as follows:

1) As discussed above, the optimal weighting coefficients of the objective function (5) are $\gamma_1 = 0.7$, $\gamma_2 = 0.3$.

2) Rated voltage is set as 1.0 pu, the first node installs the main substation, and the node voltage is set as 1.02 pu. The constraint range of node voltage is $0.9V_0 \le |V_i| \le 1.1V_0$.

3) As described in [26], it is assumed that nodes 14, 18, and 32 access DGs with a maximum generation power of 1.2 MW, distributed generators are all wind turbines, and the generating power factor of the wind turbines is 0.85,

4) It is assumed that the nodes 9, 26, and 32 access EVs, and each node accesses five electric vehicles, and the energy conversion efficiency of the charger is 0.85 [34].

4.2. Algorithm analysis and comparison

We consider each electric vehicle's maximum charging power of 200 kW and a maximum discharge power of 140 kW as an assumption [34] and use the PSO and SAPSO to optimise the example.

The parameters of the PSO are set as follows [35]: $i = 100$, $t = 200$, $c_1 = 2$, $c_2 = 2.5$ and $\omega = 0.9$. The parameters of the SAPSO are set as follows: $i = 100$, $t = 200$, $\omega_{\min} = 0.4$, $\omega_{\max} = 0.9$, $P_c = 0.5$, $P_m = 0.05$, $T = 10\,000$ and $\alpha = 0.8$. The optimisation results of the two algorithms are shown in Fig. 2. As shown in the figure, the convergence speed of the SAPSO exceeds that of the PSO, and the optimisation result of the PSO easily falls in the local optimum, and the objective function value of the PSO exceeds that of the SAPSO. The SAPSO exhibits global searching ability and possesses a significant ability to jump out of local optimal solution of SA. Thus, the SAPSO avoids the disadvantages of the PSO algorithm since it is easy to achieve local extremum. Hence, the convergence effect of the SAPSO is improved, and the optimisation effect of the SAPSO exceeds that of the PSO.

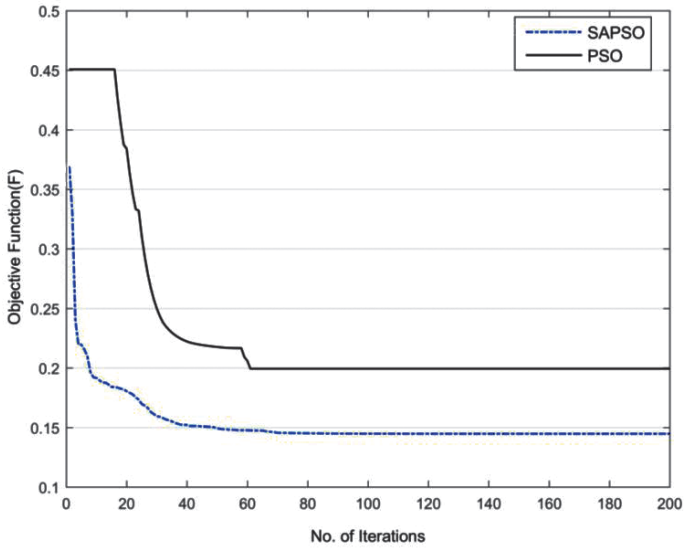

Fig. 2. Two algorithms optimization curves for 33-nodes system

4.2.1. Power loss analysis

Fig. 3 shows the change in the power loss of each branch with the aim of coordinating the DGs power generation and the charging and discharging power of the EVs while adopting different optimisation algorithms. As shown in Fig. 3, prior to the coordination and optimisation of DGs power generation and charge and discharge power of the EVs, the branch power loss is high, and the maximum branch power loss reaches 80 kW and above.

However, after coordinating and optimising the DGs power generation and charge and discharge power of the EVs with (5), the maximum power loss is less than 20 kW. Specifically, with respect to the SAPSO, the effect exceeds that in the PSO.

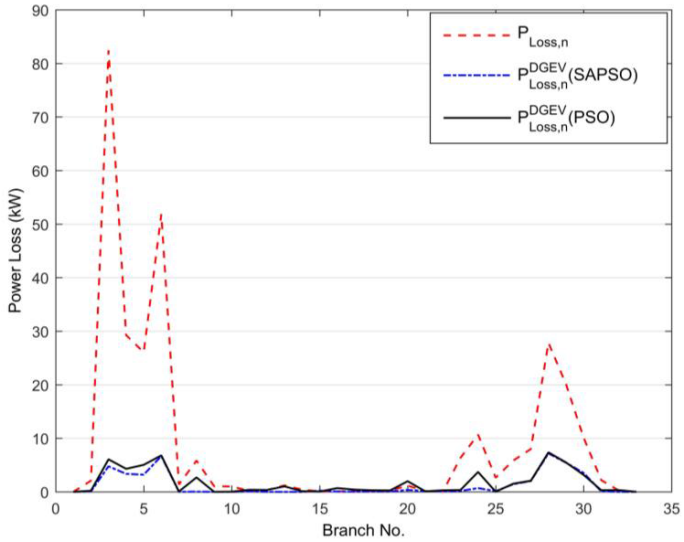

Fig. 3. Comparison of line losses with and without DGs and EVs for 33-nodes system

4.2.2. Voltage deviation analysis

Fig. 4 shows the change in the voltage deviation of each branch with the aim of coordinating the DGs power generation and the charging and discharging of EVs with different optimisation algorithms.

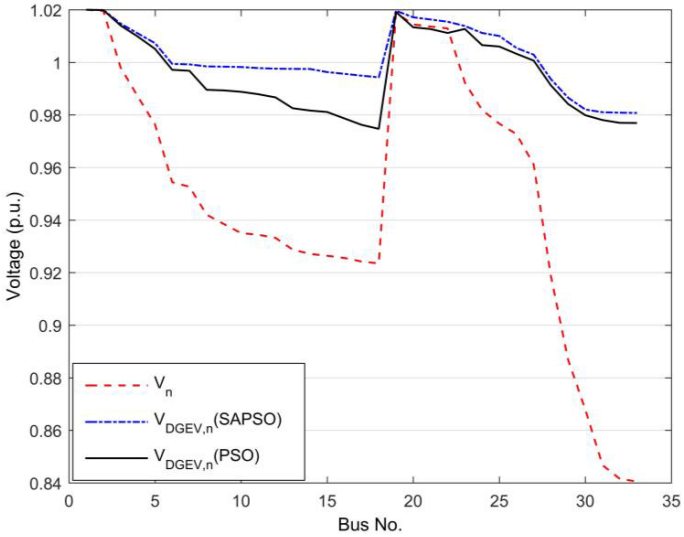

Fig. 4. Comparison of voltage magnitudes with and without DGs and EVs for 33-nodes system

From Fig. 4 it follows that before the distribution networks access DGs and EVs, the voltage deviation of each node is high, and the voltage of a few nodes is only 0.84 pu. While coordinating and optimising the DGs power generation and the charging and discharge power of the EVs, the voltage deviation of each node is lower. Specifically, with respect to the SAPSO, the voltage value of each node is in the range of 0.99 pu–1.02 pu, and the voltage deviation is the lowest.

4.2.3. Comprehensive analysis

Table 1 compares the optimisation results of the two algorithms to the optimal generation power of DGs. As shown in Table 1 the DGs power generation with SAPSO optimised is lower than that by PSO, and the k_{PLI} and the k_{VDI} are significantly reduced. When compared with the PSO, the k_{PLI} is reduced by 5.83% with the SAPSO. Thus, the power loss is reduced with the SAPSO when compared to that with the PSO. The k_{VDI} is reduced by 9.70% with the SAPSO when compared to that with the PSO. Thus, the voltage deviation is reduced with the SAPSO when compared to that with the PSO.

Table 1. Comparison of two optimization algorithms

Algorithms	**The location of DGs**	**The output power of DGs**	k_{PLI}	k_{VDI}
SAPSO	14 18 32	0.4129 0.8552 0.6012	0.1374	0.1599
PSO	14 18 32	0.5429 1.0232 0.5728	0.1957	0.2569

4.3. Analysis and comparison of two charging modes of EVs

In this section, the DGs power generation and the EVs charge power with SAPSO is coordinated and optimised by considering EVs in two charging modes. We assume that when EVs are in a slow charging mode, each EV's power is assumed in the range of 5–10 kW, and each EV's power is assumed in range of 250 kW–300 kW when it is in the fast charging mode.

4.3.1. Power loss analysis

Fig. 5 shows the power loss of every branch in distribution networks before DGs and EVs access and that of every branch with two charging modes of EVs.

As shown in Fig. 5, the branch power loss is high before the coordination and optimisation of DGs power generation and EVs charging power. The branch of the power loss is reduced after coordinating and optimising the DGs power generation and EVs charging power. Specifically, when the EVs are in the slow charging mode, the branch of the power loss decreases, and the maximum loss is less than 10 kW.

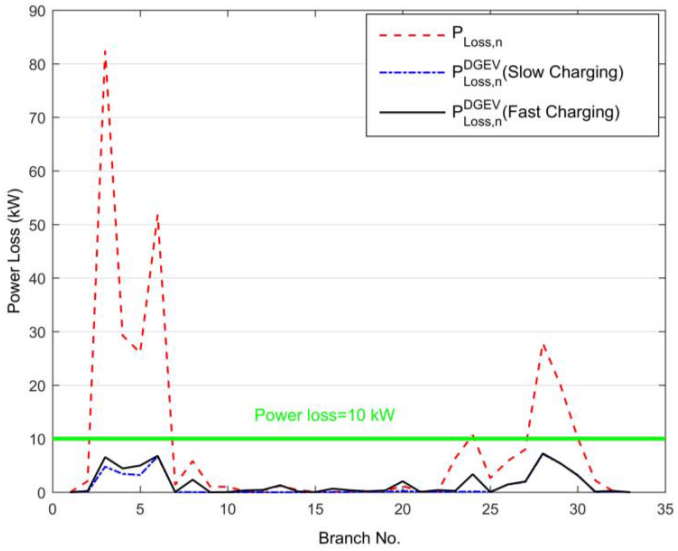

Fig. 5. Comparison of the line losses in two charging modes for 33-nodes system

4.3.2. Voltage deviation analysis

Fig. 6 shows the voltage deviation of every node when EVs are in two charging modes.

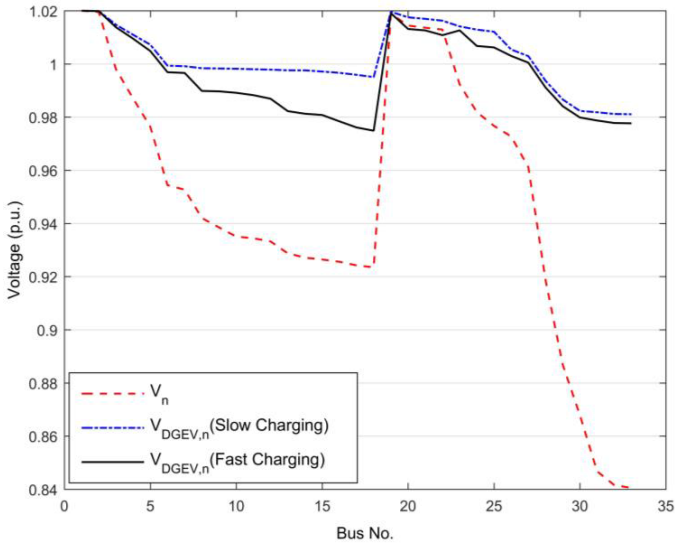

Fig. 6. Comparison of the voltage magnitude in two charging modes for 33-nodes system

As shown in Fig. 6, the voltage deviation is the same as that shown in Fig. 4 before DGs and EVs access the distribution networks. After coordinating and optimising the power generation of DGs and the charging power of EVs, the voltage deviation of each node is reduced, and this

is within the allowable voltage deviation range of the distribution networks. However, the EVs' charging power is high when the EVs are in the fast charging mode. It is observed that the 30–33 node voltage is slightly lower than 0.98 pu. Conversely, when the EVs are in the slow charging mode, the voltage of each node is within the range of 0.99 pu–1.02 pu.

4.3.3. Comprehensive analysis

Table 2 shows a comparison of the DGs optimal power generation with the two charging modes of the EVs. When the EVs are in the slow charging mode, the output powers of DGs, namely k_{PLI} and k_{VDI}, are smaller than those in the fast charging mode. When compared with fast charging mode, the k_{PLI} is reduced by 11.57% in the slow charging mode. Thus, the power loss is reduced in the slow charging mode when compared with that in the fast charging mode. The k_{VDI} is reduced by 6.44% in the slow charging mode when compared with that in the fast charging mode. Thus, the voltage deviation is reduced in the slow charging mode when compared with that in the fast charging mode.

Table 2. Comparison of optimal power of DGs based on two charging methods of EVs

The charging mode	**The location of DGs**	**The output power of DGs**	k_{PLI}	k_{VDI}
Slow charging mode	14 18 32	0.3953 0.6846 0.5573	0.1276	0.1664
Fast charging mode	14 18 32	0.8239 1.1123 1.0532	0.2433	0.2308

4.4. Analysis and comparison of simulation with large scale EVs

To validate the proposed methodology, the code of SAPSO was also implemented on a larger scale 118-nodes radial distribution system without tie-lines with a larger scale EVs. The detailed data of the 118-nodes radial distribution system is given in [36]. The active power, reactive power, and resistance of each node in the system are per unit values and related to the capacity and the voltage. It is assumed that in slowing charging mode the nodes 3, 10, 18, 23, 42, 54, 65, 68, 88 and 116 access EVs, and each node accesses 100 electric vehicles, the energy conversion efficiency of the charger is 0.85. However in fast charging mode there are only 500 EVs installed at the nodes 3, 5, 45, 62, 70, 79, 90, 106 and 110. Because when insalled with thousands of EVs the 118-nodes distribution networks will almost collapse in fast charging. DG units are installed at nodes 28, 35, 57, 77, 88 and 113 which are more sensitive to loss sensitivity factor in the system [37]. The capacity of the DG of renewable energy systems is 3.0 MW and the power factor of which is 0.95. The assumptions and the parameters of the SAPSO are shown as Section 4.2. Fig. 7 shows the convergent curve of SAPSO. The number of iterations is 100 in 118-nodes system while the number of iterations of SAPSO is only 70 in 33-nodes system. And the iteration time is 103 s in 118-nodes distribution networks while the iteration time in 33-nodes distribution networks is only 11 s. That means that with the increasing number of nodes and electric vehicles, the computational complexity and the execution time will increase.

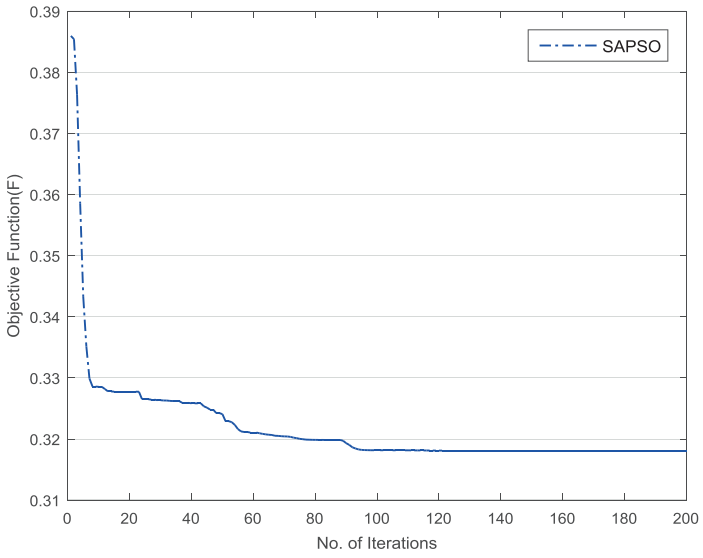

Fig. 7. Convergent curve of SAPSO for 118-nodes system

4.4.1. Power loss analysis

Fig. 8 shows the power loss of every branch in 118-nodes distribution networks with large scale EVs in two charging modes. Obviously, the power loss of every branch in distribution networks has great changed in the fast charging mode. The maximum branch power loss is almost

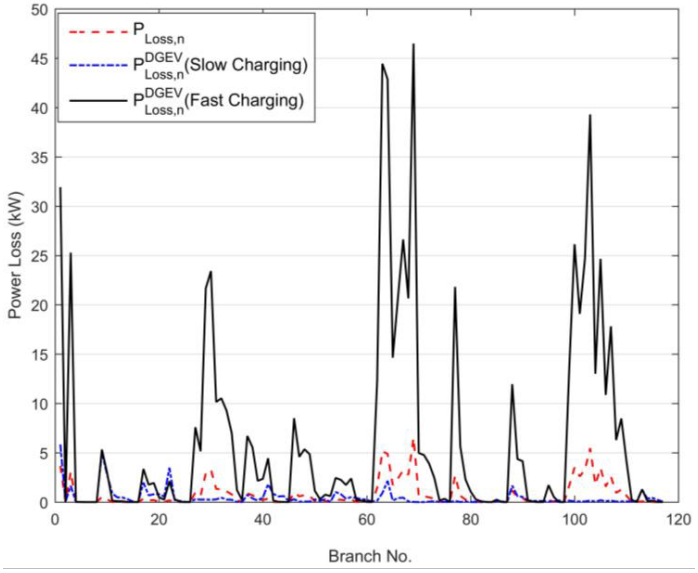

Fig. 8. Comparison of the line losses in two charging modes for 118-nodes system

up to 50 kW. However, it can also be seen from Fig. 8 that the simulated results do not have much change in a slow charging mode. The maximum power loss is less than 10 kW.

4.4.2. Voltage deviation analysis

Fig. 9 shows the voltage deviation of every node in 118-nodes distribution networks with large scale EVs in two charging modes. Obviously, the voltage deviation of every node has great changes in the fast charging mode. The maximum voltage deviation is almost below 0.94 pu, which is almost beyond the permitted scope of the distribution network. At the same time, it can also be seen from Fig. 9 that the simulated results do not show much change in a slow charging mode.

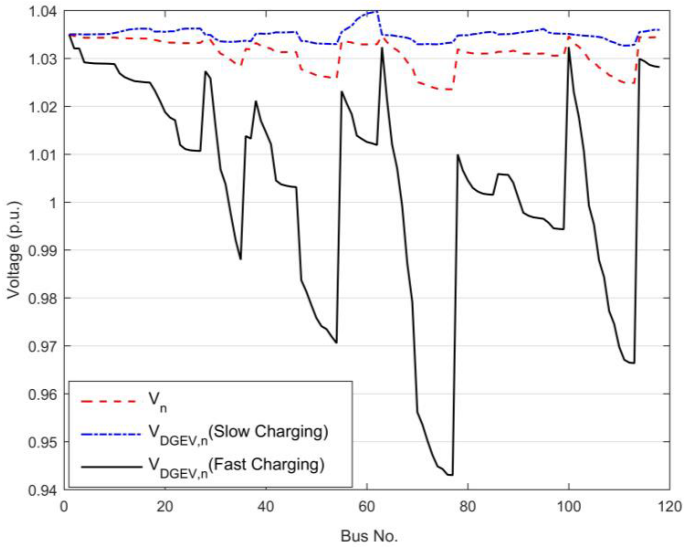

Fig. 9. Comparison of the voltage magnitude in two charging modes for 118-nodes system

5. Conclusion

In the study, the authors considered the access of DGs and EVs to the distribution networks. Subsequently, the power generation of DGs and charging and discharging power of EVs were optimised via multi-objective coordination. The minimums of the *PLI* and *VDI* were selected as the multi-objective functions. The proposed scheme was tested on IEEE 33-nodes distribution systems and IEEE-118 nodes large scale distribution systems to minimise the losses and to improve the voltage profile. In IEEE 33-nodes distribution systems, the simulated results obtained via SAPSO were compared with the PSO results. The optimisation results indicated that the effect of the SAPSO exceeds that of the PSO. With the SAPSO, the system efficiency significantly improved when EVs were in the slow charging mode when compared with that in the fast charging mode in IEEE 33-nodes distribution systems with small scale EVs and in IEEE-118 nodes large scale

distribution systems with thousands of EVs. The results show that with the methodology supposed in this paper thousands of EVs can access the distribution network in a slow charging mode.

Acknowledgements

Authors gratefully acknowledge the support of the National Natural Science Foundation of China (50767001); Natural Science Foundation of Guangdong (S2013010012431, 2014A030313509); Guangdong special fund for public welfare study and ability construction (2014A010106026); The Talent Introduction Special Foundation Project of Guangdong High School.

References

[1] Liu B.L., Huang X.L., Li J. *et al*., *Multi-objective planning of distribution networks containing distributed generation and electric vehicle charging stations*, Power System Technology, vol. 39, no. 2, pp. 450–456 (2015).

[2] Pantos M., *Exploitation of electric-drive vehicles in electricity markets*, IEEE Transactions on Power Systems, vol. 27, no. 2, pp. 682–694 (2012).

[3] Denysiuk S., Derevianko D., *A novel method of complex reliability assessment in microgrids with distributed generation*, International Conference on Modern Electrical and Energy Systems (MEES), Kremenchuk, Ukraine, pp. 212–215 (2017).

[4] Moradi M., Abedini M., *A combination of genetic algorithm and particle swarm optimization for optimal DG location and sizing in distribution systems*, International Journal of Electrical Power and Energy Systems, vol. 34, no. 1, pp. 66–74 (2012).

[5] Abdi Sh., Afshar K., *Application of IPSO-monte carlo for optimal distributed generation allocation and sizing*, International Journal of Electrical Power and Energy Systems, vol. 44, no. 1, pp. 786–797 (2013).

[6] Devi S., Geethanjali M., *Application of modified bacterial foraging optimization algorithm for optimal placement and sizing of distributed generation*, Expert Systems with Applications, vol. 41, no. 6, pp. 2772–2781 (2014).

[7] Zakariazadeh A., Jadid S., Siano P., *Integrated operation of electric vehicles and renewable generation in a smart distribution system*, Energy Conversion and Management, vol. 89, no. 1, pp. 99–110 (2015).

[8] Liu Z.P., Wen F.S., Xue Y.S. *et al*., *Optimal siting and sizing of electric vehicle charging station*, Automation of Electric Power Systems, vol. 36, no. 3, pp. 54–59 (2012).

[9] Deilami S., Masoum A.S., Moses P.S. *et al*., *Real-time coordination of plug-in electric vehicle charging in smart grids to minimize power losses and improve voltage profile*, IEEE Trans on Smart Grid, vol. 2, no. 3, pp. 456–467 (2011).

[10] Bourass A., Cherkaoui S., Khoukhi L., *Secure optimal itinerary planning for electric vehicles in the smart grid*, IEEE Transactions on Industrial Informatics, vol. 13, no. 6, pp. 3236–3245 (2017).

[11] Bashiri M., Bahadori N., *Optimized plan of charging stations for management of demands: An emerging need of hybrid electric vehicle*, Future Technologies Conference, San Francisco, CA, USA, pp. 422–425 (2016).

[12] Zhang J., Zhou H., Li H. *el at*., *Multi-objective planning of charging stations considering vehicle arrival hot map*, IEEE Conference on Energy Internet and Energy System, Beijing, China, pp. 1–6 (2017).

[13] Nafisi H., Agah S.M.M., Abyaneh H.A. *el at*., *Two-stage optimization method for energy loss minimization in microgrid based on smart power management scheme of PHEVs*, IEEE Transactions on Smart Grid, vol. 7, no. 3, pp. 1268–1276 (2016).

[14] Cheng L., Chang Y., Huang R.L., *Mitigating voltage problem in distribution system with distributed solar generation using electric vehicles*, IEEE Transactions on Sustainable Energy, vol. 6, no. 4, pp. 1475–1484 (2015).

[15] Abdelsamad S.F., Morsi W.G., Sidhu T.S., *Impact of wind-based distributed generation on electric energy in distribution systems embedded with electric vehicles*, IEEE Transactions on Sustainable Energy, vol. 6, no. 1, pp. 79–87 (2015).

[16] Jiang X.L., Wang J.K., Han Y.H. *et al*., *Coordination dispatch of electric vehicles charging/discharging and renewable energy resources power in microgrid*, Procedia Computer Science, vol. 107, no. 4, pp. 157–163 (2017).

[17] Paterakis N.G., Erdinç I., Bakirtzis A.G., *Coordinated operation of a neighborhood of smart households comprising electric vehicles, energy storage and distributed generation*, IEEE Transactions on Smart Grid, vol. 7, no. 6, pp. 2736–2747 (2016).

[18] Ahmadian A., Sedghi M., Aliakbar-Golkar M., *Fuzzy load modelling of plug-in electric vehicles for optimal storage and DG planning in active distribution networks*, IEEE Transactions on Vehicular Technology 2017, vol. 66, no. 5, pp. 3622–3631 (2017).

[19] Chu C.C., Tsai M.S., *Application of novel charged system search with real number string for distribution system loss minimization*, IEEE Transactions on Power Systems, vol. 28, no. 4, pp. 3600–3609 (2013).

[20] Li Z.K., Tian Y., Dong C.M. *et al*., *Distributed generators programming in distribution networks involving vehicle to grid based on probabilistic power flow*, Automation of Electric Power Systems, vol. 38, no. 16, pp. 60–66 (2014).

[21] Chen G., Dai P., Zhou H. *et al*., *Distribution system reconfiguration considering distributed generators and plug-in electric vehicles*, Power System Technology, vol. 37, no. 1, pp. 82–88 (2013).

[22] Liu B.L., Huang X.L., Li J. *et al*., *Multi-objective planning of distribution network containing distributed generation and electric vehicle charging stations*, Power System Technology, vol. 39, no. 2, pp. 450–456 (2015).

[23] Zeng B., Li Y.Z., Feng J.H. *et al*., *A combinatorial planning method for distributed generation and intelligent parking lots considering reactive supporting capability of electric vehicles*, Transations of China Electrotechnical Society, vol. 32, no. 23, pp. 185–197 (2017).

[24] Awasthi A., Venkitusamy K., Padmanaban S. *et al*., *Optimal planning of electric vehicle charging station at the distribution system using hybrid optimization algorithm*, Energy, vol. 155, no. 8, pp. 70–78 (2017).

[25] Mohamed I.A., Kowsalya M., *Optimal size and sitting of multiple distributed generators in distribution system using bacterial foraging optimization*, Swarm and Evolutionary Computation, vol. 15, no. 4, pp. 58–65 (2014).

[26] Singh D., Singh D., Verma K.S., *Multiobjective optimization for DG planning with load models*, IEEE Transactions on Power Systems, vol. 24, no. 1, pp. 427–436 (2009).

[27] Sahraei-Ardakani M., Peydayesh M., Rahimi-Kian A., *Multi attribute optimal DG planning under uncertainty using AHP method*, Proceedings of IEEE PES General meeting on Conversion and Delivery of Electrical Energy in the 21st Century, Pittsburgh, USA, pp. 1–5 (2008).

[28] Jin J., Rothrock L., McDermott P.L. *et al*., *Using the analytic hierarchy process to examine judgment consistency in a complex multiattribute task sign in or purchase*, IEEE Transactions on Systems, Man, and Cybernetics-Part A: Systems and Humans, vol. 40, no. 5, pp. 1105–1115 (2010).

[29] Guo Q.Y., Wu J.K., Mo C. *et al*., *A model for multi-objective coordination optimization of voltage and reactive power in distribution networks based on mixed integer second-order cone programming*, Proceedings of the Chinese Society for Electrical Engineering, vol. 38, no. 5, pp. 1385–1396 (2017).

[30] Liu Z.P., Wen F.S., Gerard L., *Optimal siting and sizing of distributed generators in distribution systems considering uncertainties*, IEEE Transactions on Power Delivery, vol. 26, no. 4, pp. 2541–2551 (2011).

[31] Kennedy J., Eberhart R., *Particle swarm optimization*, IEEE International Conference on Neural Networks, Perth, Australia, pp. 1942–1948 (1995).

[32] Li X.B., Zhu Q.J., *Application of improved particle swarm optimization algorithm to multi-objective reactive power optimization*, Transactions of China Electrotechnical Society, vol. 25, no. 7, pp. 137–143 (2010).

[33] Kirkpatrick S., Gelatt C.D., Vecchi M.P., *Optimization by simulated annealing*, Science, vol. 220, no. 4598, pp. 671–680 (1983).

[34] Li H.M., Cui H.T., Wan Q.L., *Distribution network reconfiguration based on second-order conic programming considering EV charging strategy*, Proceedings of the Chinese Society for Electrical Engineering, vol. 35, no. 18, pp. 4674–4681 (2015).

[35] Wu J.K., Xiong Y., *Establishment and solution of the complementary power generation model of wind-energy, hydro-energy and natural gas*, Power System Technology, vol. 38, no. 3, pp. 603–609 (2014).

[36] Zhang D., Fu Z.C., Zhang L.C., *An improved TS algorithm for loss minimum reconfiguration in large-scale distribution systems*, Electric Power Systems Research, vol. 77, no. 5–6, pp. 685–694 (2007).

[37] Injeti S.K., Kumar N.P., *A novel approach to identify optimal access point and capacity of multiple DGs in a small, medium and large scale radial distribution systems*, Electric Power Energy Systems, vol. 45, no. 1, pp. 142–151 (2013).